

Supporting Information

Pseudo metal generation via catalytic oxidative polymerization on the surface of reactive template for redox switched off-on photothermal therapy

Seo Ryung Bae,^a Jihye Choi,^a Hyun-Ouk Kim,^a Byunghoon Kang,^a Myeong-Hoon Kim,^a Seungmin Han,^a Ilkoo Noh,^a Jong-Woo Lim,^a Jin-Suk Suh,^b Yong-Min Huh^b and Seungjoo Haam^a

^aDepartment of Chemical and Biomolecular Engineering, College of Engineering, Yonsei University, Seoul 120-749, Republic of Korea, E-mail: haam@yonsei.ac.kr

^bDepartment of Radiology, College of Medicine, Yonsei University, Seoul 120-752, Republic of Korea, E-mail: ymhuh@yuhs.ac

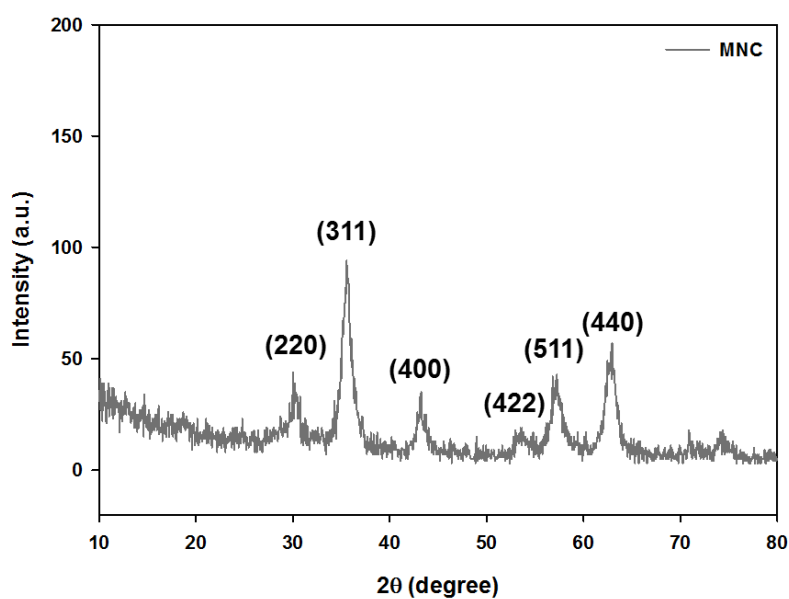


Fig. S1 XRD pattern of MNC.

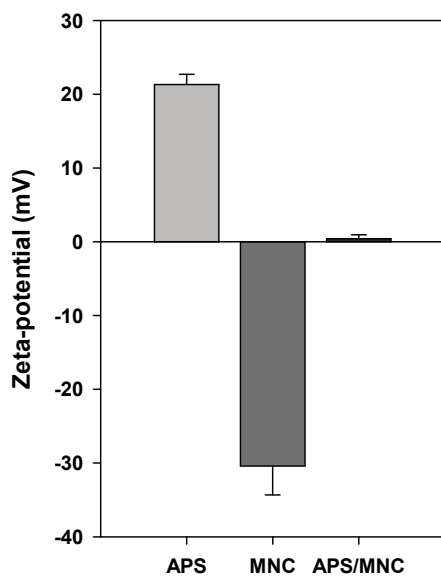


Fig. S2 Zeta-potential of APS, MNC, and APS/MNC.

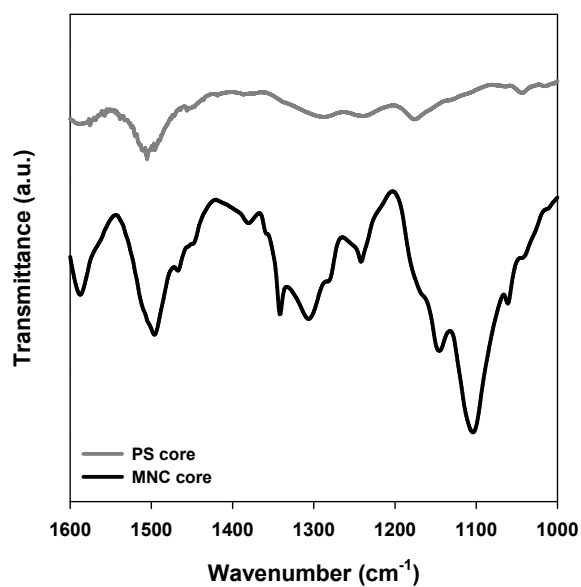


Fig. S3 FT-IR spectra of PMP and PS with aniline polymerized with an excess amount of APS (228 mg). The typical PANI peak at 1,130 cm^{-1} is not shown, which indicates that aniline was not polymerized into PANI on the surface of polystyrene.

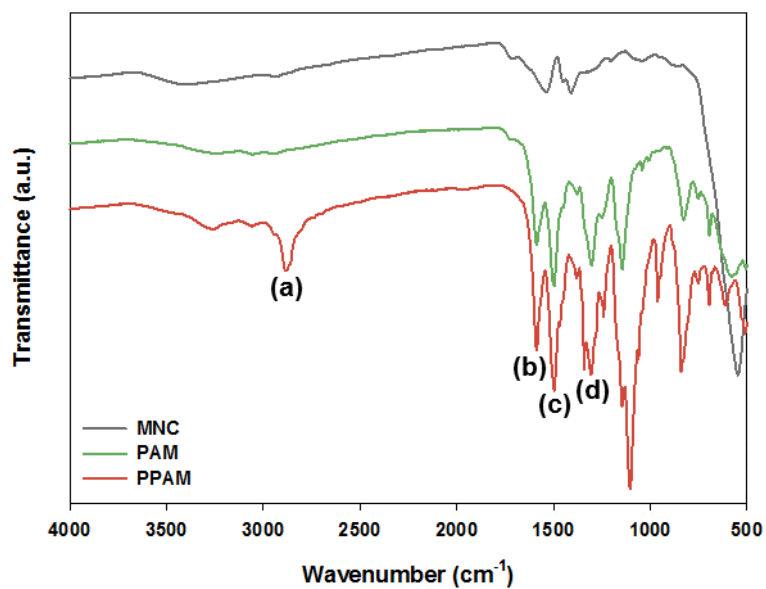


Fig. S4 FT-IR spectra of MNC, PAM, and PPAM showing (a) -CH- stretching of mPEG, (b) C=C stretching of quinoid rings, (c) C=C stretching of benzenoid rings, and (d) C-N stretching of aromatic amine.

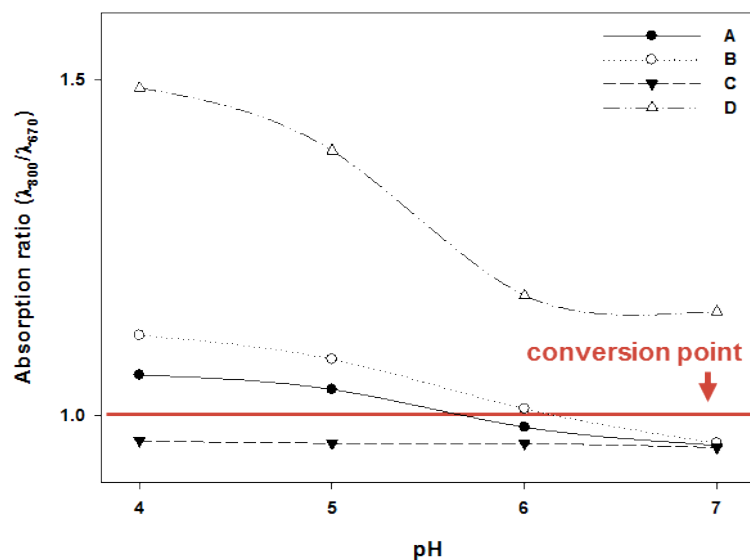


Fig. S5 Absorption ratio of PPAMs synthesized with various APS and Fe ion concentration ratios at four different pH values, showing the absorbance shift between EB and ES states. PPAM synthesized with an excess amount of APS (entry C) was doped to ES at pH 2, whereas PPAM synthesized with a minimal amount of APS (entry A) reveals an EB-ES conversion point between pH 5 and 6. A similar result is shown for entry B. By increasing the concentration of participating IOGs (entry D), the transition point was alkaline-shifted.

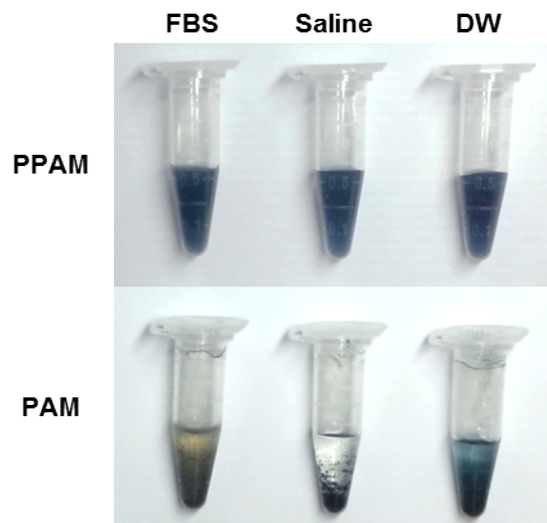


Fig. S6 Photographs of PPAM and PAM dispersed in FBS, saline, and DW for longer than one month.

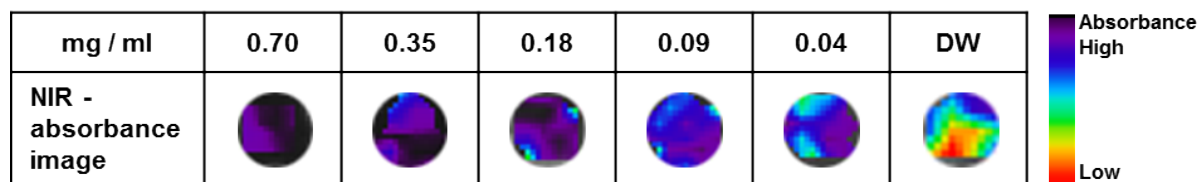


Fig. S7 Near-infrared (NIR) absorption images of PPAMs at different concentrations in aqueous solutions.

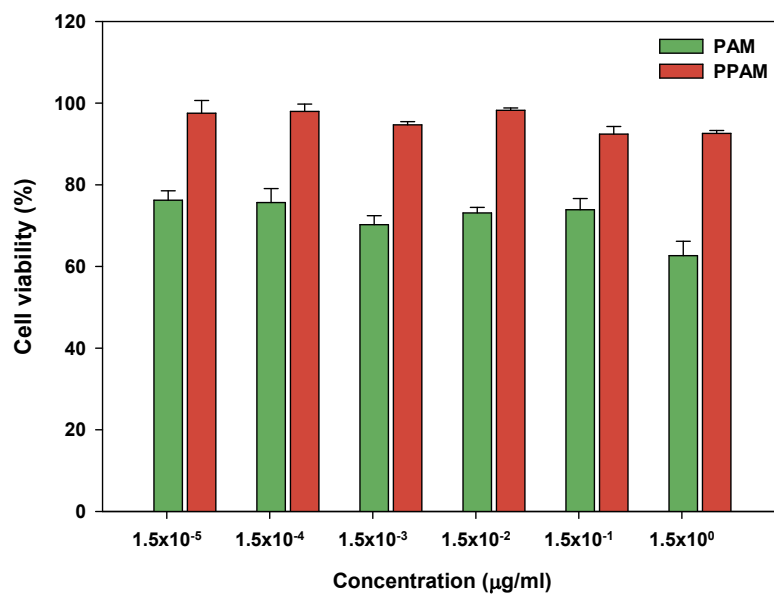


Fig. S8 Cell viabilities of HT1080 cells after incubation with treatments of PAMs and PPAMs of various concentrations.

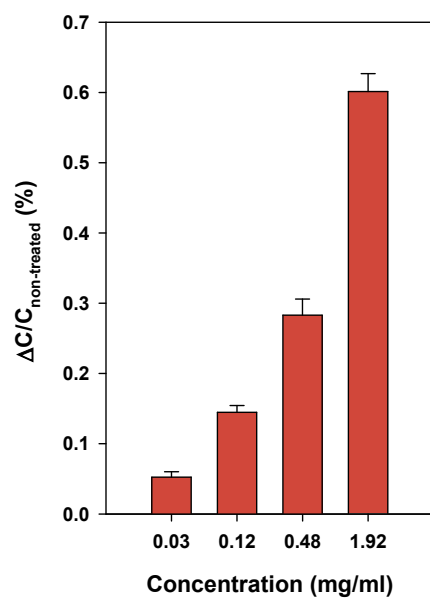


Fig. S9 The relative concentrations (%) of HT1080 cells after treatment of PPAM versus non-treated HT1080 cells through comparison of the Fe concentration using ICP-OES analysis.

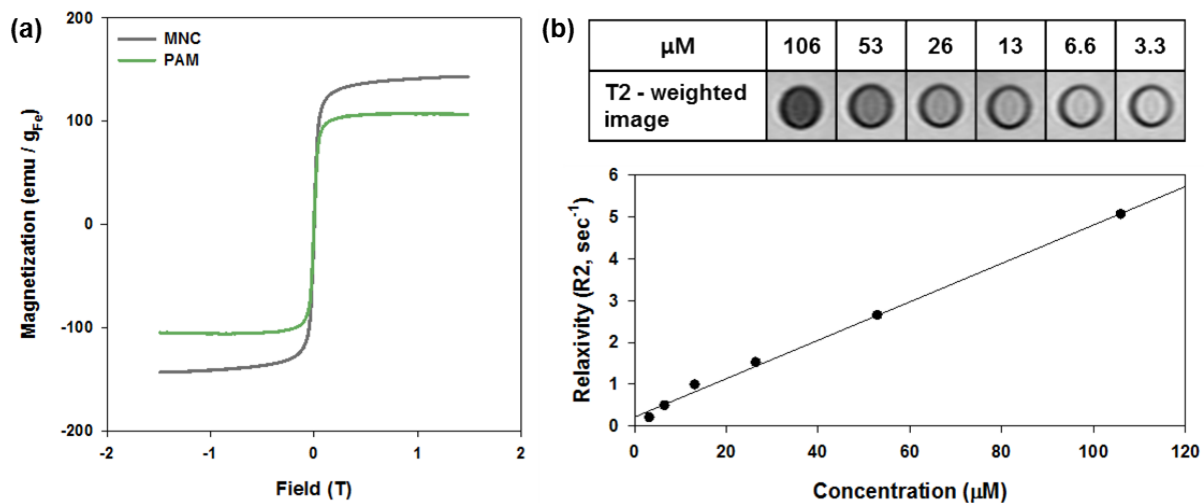


Fig. S10 (a) Magnetic hysteresis loops of MNC and PAM. (b) T2-weighted MR images and relaxivity (R2) graph of PPAM at various concentrations.